Eur. Phys. J. Plus (2023) 138:846
https://doi.org/10.1140/epjp/s13360-023-04501-4

THE EUROPEAN PHYSICAL JOURNAL PLUS

Regular Article

Particle acceleration and thermodynamics of the rotating Simpson–Visser black hole

Abdurakhmon Nosirov[1,2,a], **Farruh Atamurotov**[3,4,5,6,b], **Gulzoda Rakhimova**[7,c], **Ahmadjon Abdujabbarov**[1,2,7,d]

[1] National University of Uzbekistan, 100174 Tashkent, Uzbekistan
[2] Ulugh Beg Astronomical Institute, Astronomy St 33, 100052 Tashkent, Uzbekistan
[3] New Uzbekistan University, Mustaqillik ave. 54, 100007 Tashkent, Uzbekistan
[4] Central Asian University, Milliy Bog' Street 264, 111221 Tashkent, Uzbekistan
[5] Inha University in Tashkent, Ziyolilar 9, 100170 Tashkent, Uzbekistan
[6] Institute of Fundamental and Applied Research, National Research University TIIAME, Kori Niyoziy 39, 100000 Tashkent, Uzbekistan
[7] Tashkent State Technical University, 100095 Tashkent, Uzbekistan

Received: 21 June 2023 / Accepted: 15 September 2023

Abstract We have considered a time-like geodesics in the background of rotating Simpson–Visser (SV) black hole (BH) to examine structure of the horizon and ergosphere. The innermost stable circular orbits (ISCO) and the effective potential, which controls the particle's motion in spacetime, have been studied for different values of parameters in SV BH. Center-of-mass (CM) energy of two colliding particles near the horizon has been investigated for both extremal and non-extremal cases. Furthermore, thermodynamic properties of SV black hole have been also investigated in detail.

1 Introduction

The general relativity (GR) is a part of standard model describing the gravitational interaction. GR has been justified via the observation of gravitational lensing of photons near the Sun detected during the solar eclipse in 1919 [1, 2] just after its proposal by Einstein in 1915 [3]. Later GR has been several times well tested in weak (e.g., using solar system tests [4]) and strong field regimes (e.g., gravitational wave observation [5] and observation of shadow of black holes (BHs) [6, 7]). Besides, Authors of Refs. [8, 9] provide more stringent constraints on possible deviations from the Kerr solution than GWs and shadow. At the same time, GR meets some fundamental problems related to, for example, the existence of the singularity at the origin of vacuum solutions, etc. There is strong belief that these issues may be resolved by introducing the modifications or alternatives to the standard theory of gravity.

Any modifications/alternates to standard theories have to be probed using experimental and observational data. However, the big number of modified and alternative theories of gravity create additional degeneracy problem: the effects due to parameters of different models may mimic each other. In order to resolve one may consider several independent experiments/observations [10, 11] or use the parameterization [12, 13].

Authors of Ref. [14] have proposed very interesting approach to generalize the Kerr BH solution into regular rotating Kerr-like (or rotating SV) one. This new regular Kerr-like solution contains asymptotically Minkowski core. Optical properties of this Kerr-like regular spacetime has been studied in [15]. The non-rotating case of this regular BH solution has been analyzed in [16]. The geodesic properties of spherical-symmetric regular spacetime containing asymptotically Minkowski core have been explored in Ref. [17]. Particularly, gravitational lensing effect in the weak field regime around Schwarzschild-like BH has been studied in Ref. [18] in the presence of plasma. Here, we plan to explore the thermodynamics, energetic properties and dynamics of rotating SV BH.

One of the most prominent way to test the metric theory of gravity is exploration of particle dynamics [19–24]. Especially, the dynamics of the charged test particles become very sensitive to external electromagnetic field [25–27]. One may find interesting works where test particles with nonvanishing electric and/or magnetic charges dynamics have been explored in detail [28–42]. Authors of Ref. [19] have shown that extreme rotating Kerr BH can play a role of accelerator of particles. Particularly, for the fine-tuned value of the particle's angular momentum the center of mass energy diverges at the horizon. The effect of other parameters

[a] e-mail: abdurahmonnosirov000203@gmail.com
[b] e-mail: atamurotov@yahoo.com (corresponding author)
[c] e-mail: phisic_96@mail.ru
[d] e-mail: ahmadjon@astrin.uz

Published online: 25 September 2023

of rotating BH in different gravity models have been discussed in Refs. [43–48]. Magnetic field around no-rotating BH may mimic the effect of rotation and accelerate the charged particles [49–53].

The study of the BH thermodynamics is directly related to the properties of the entropy of the BH. The pioneering works on thermodynamic properties of BH can be found in Refs. [54–56]. Surely, the simplest BH solution is described by the Schwarzschild spacetime metric and the entropy and related thermodynamic properties of this type of BH have been explored in [57–59]. Particle spectrum and some thermodynamical properties of Reissner–Nordström BH have been studied in [60]. The thermodynamics of a magnetically charged regular BH obtained using the action of general relativity and nonlinear electromagnetics has been studied in [61]. The effects of quintessence on thermodynamics of BH have been analyzed in [62]. The thermodynamic properties of BH in Hořava–Lifshitz gravity have been explored in Refs. [63, 64]. Thermodynamic properties and Joule–Thomson expansion for conical or BTZ-like BH is investigated in [65]. Besides, several works are studied regarding thermodynamics of non-rotating and rotating black hole in detail in Refs. [66–72].

Here, we plan to study the particle dynamics, acceleration process, and thermodynamic properties of rotating SV BH. The current work is organized as follows: we start with the short description of the Kerr-like spacetime metric in Sect. 2. The equations of motion of test particles have been explored in Sect. 3. The acceleration of test particles near the horizon of rotating SV BH is studied in Sect. 4. Finally, we discuss the thermodynamic properties of the rotating SV BH in Sect. 5. We conclude our results in Sect. 6. Here, we use the geometrized unit of system where gravitational constant G and vacuum speed of light c set to unity. For the spacetime signature we use $(-, +, +, +)$.

2 Rotating Simpson–Visser black hole

The gravitational field of a rotating Simpson–Visser compact object in Boyer–Lindquist coordinates can be expressed through the following line element [14, 15]

$$ds^2 = -\frac{\Delta}{\rho^2}(dt - a\sin^2\theta d\phi)^2 + \frac{\rho^2}{\Delta}dr^2 + \rho^2 d\theta^2 + \frac{\sin^2\theta}{\rho^2}\big(adt - (r^2+a^2)d\phi\big)^2, \tag{1}$$

with the metric functions defined as

$$\rho^2 = r^2 + a^2\cos^2\theta, \tag{2}$$

$$\Delta = r^2 + a^2 - 2Mre^{-l/r}, \tag{3}$$

where a and l can be referred as spin and deviation parameters of SV BH, respectively. This metric is derived from regularization procedure in Kerr metric like did in Schwarzschild metric before where $M \to M(r) = Me^{-l/r}$ modification is done. Here, l can be viewed as quantifying the deviation from Kerr. The spacetime around this black hole behaves as one around typical rotating and the limit $l \to 0$ corresponds to Kerr BH. Furthermore, mathematically there is still a discontinuity at $r = 0$ and it maintains asymptotically flatness as $r \to +\infty$.

The Kerr-like BH described by the spacetime metric (1) need to be investigated to possess the horizon structure and the ergosphere region, likewise the other rotating BHs. We aim to examine the properties of the above indicated features depending on the spin parameter a and the deviation parameter l. Figure 1 clearly shows the regions in $a - l$ plane corresponding to BH and No black hole cases. The radii of the *Cauchy horizon* r_H^- and the *event horizon* r_H^+ are attained by $\Delta = 0$ corresponding to the coordinate singularity. The BH turns out to be an *extremal* BH when the two horizons coincide for a specific critical spin parameter (deviation parameter) $a = a_E$ $(l = l_E)$, whereas $a < a_E$ $(l < l_E)$ refers to a *non-extremal* BH with two distinct horizons. Figures 2 and 3 show the behavior of horizons by varying the spin parameters a and l. These figures imply that for $a < a_E$ or $l < l_E$ there exit a set of values of parameters for which one can get two horizons and when $a = a_E$ or $l = l_E$ these horizons collide, i.e., we have an extremal BH with degenerate horizons (cf. Table 1). Particularly, in Table 1, we have presented the numerical values of the radius of horizons and their difference for different values of l and a. It can be noticed that with the rise of these two parameters, horizons come closer to each other. In the case of $a > a_E$ or $l > l_E$ there is no BH because no horizon appears in that particular case. Moreover, the BH admits two static limit surfaces r_{sls}^- and r_{sls}^+, which are the positive real roots of equation $g_{tt} = 0$. In Fig. 4, we depict possible solutions of this equation with different combinations of the parameters of a and l and different values of θ. Observing the outer event horizon and the stationary limit surface of this BH, it is verified that the stationary limit surface always lies outside of event horizon for all values of l. The region, i.e., $r_H^+ < r < r_{sls}^+$ connotes the *ergosphere* region and its boundary r_{sls}^+ is called the *static limit surface*. Its shape is that of an oblate spheroid-bulging at the equator and flattened at the poles of the rotating BH. We have studied how the parameters a and l affect the shape of the ergosphere. The behavior of ergospheres for $a < a_E$ and $a \approx a_E$ are shown in Fig. 5. It can be seen that the ergospere is sensitive to the parameter l, meaning that with the increase of parameter l, the thickness of ergosphere also increases. The same is true for spin parameter a, as well.

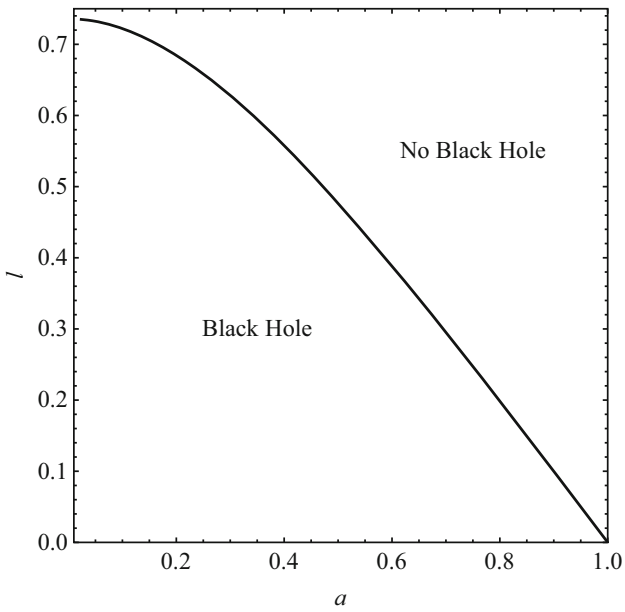

Fig. 1 Plot showing the behavior of the spin parameter a and a deviation parameter l of Kerr-like BH. The *solid line* is the boundary, which separates the BH region from the no BH region. Here $M = 1$

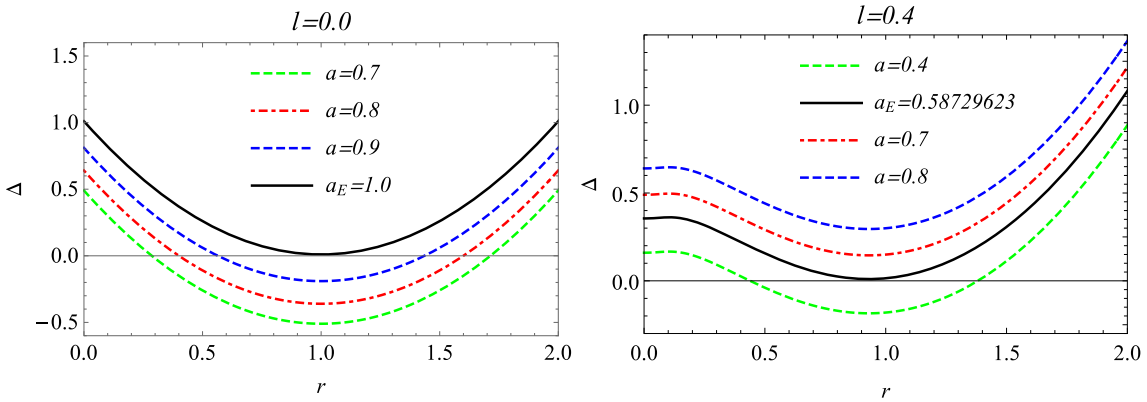

Fig. 2 Plot showing the behavior of Δ with respect to r for different values of l. The case $a = a_E$ corresponds to an extremal BH. Here $M = 1$

3 Equations of motion and effective potential in an equatorial plane

Here, we consider motion of a time-like particle with a rest mass m_0 in the equatorial plane $\theta = \pi/2$ where the polar velocity $\dot{\theta}$ becomes zero. The metric and generalized momenta of the particle in the spacetime of a rotating BH is expressed in the form,

$$P_t = g_{tt}\dot{t} + g_{t\phi}\dot{\phi}, \tag{4}$$

$$P_\phi = g_{\phi\phi}\dot{\phi} + g_{t\phi}\dot{t}, \tag{5}$$

where P_t and P_ϕ are the constants of motion. Basically, the two quantities P_t and P_ϕ correspond to the particle's energy $-E$ and the angular momentum L, respectively. The overdot denotes differentiation with respect to the proper time. The equations of motion of a massive particle are calculated from Eqs. (4)–(5) along with the normalization condition $u_\mu u^\mu = -1$, given as below

$$\dot{t} = \frac{1}{r^2}\left[\frac{(a^2+r^2)}{\Delta}(E(a^2+r^2) - aL) + a\left(L - aE\right)\right], \tag{6}$$

$$\dot{\phi} = \frac{1}{r^2}\left[\frac{a}{\Delta}(E(a^2+r^2) - aL) + \left(L - aE\right)\right], \tag{7}$$

$$\dot{r} = \pm\frac{\sqrt{(aL - (a^2+r^2)E)^2 - \Delta(m_0^2 r^2 + (L - aE)^2)}}{r^2}. \tag{8}$$

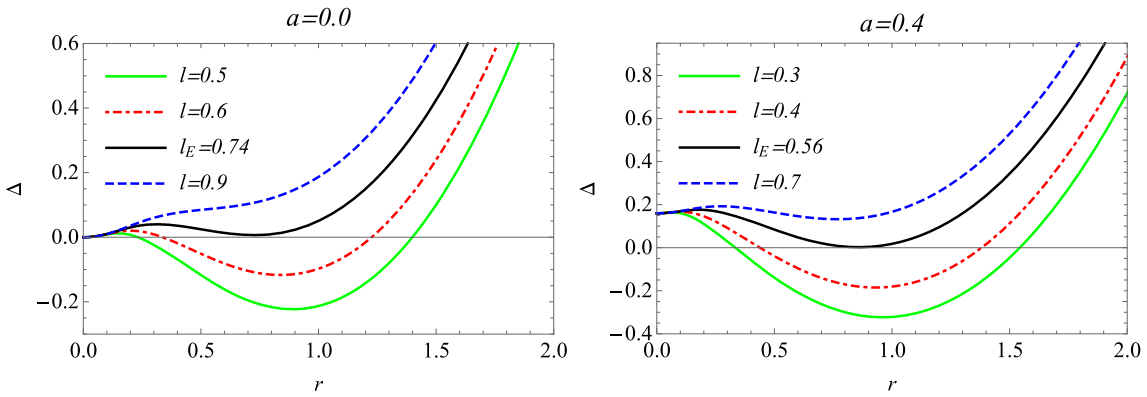

Fig. 3 Plot showing the behavior of Δ with respect to r for different values of a. Here $M = 1$

Table 1 The values of the horizons of a rotating SV BH with the parameter M=1 ($\delta_e^g = r_{sls}^+ - r_H^+$). $a_E^* = 1, 0.7986107603743899, 0.6950554457736542$ and 0.5872962339024399, which, respectively, corresponds to l=0, 0.2, 0.3 and 0.4

a	$l=0$			$l=0.2$			$l=0.3$			$l=0.4$		
	r_H^-	r_H^+	δ_e^g	r_H^-	r_H^+	δ_e^g	r_H^-	r_H^+	δ_e^g	r_H^-	r_H^+	δ_e^g
0.4	0.0834	1.9165	1.8331	0.2481	1.6804	1.4323	0.3334	1.5428	1.2094	0.4385	1.3813	0.9427
0.5	0.1339	1.8669	1.7321	0.3289	1.6114	1.2824	0.4382	1.4558	1.0175	0.5882	1.2548	0.6666
0.6	0.2	1.8	1.6	0.43487	1.5151	1.0801	0.5875	1.3213	0.7337	–	–	–
0.7	0.2858	1.7141	1.4282	0.5863	1.3712	0.7848	–	–	–	–	–	–
a_E^*	1	1	0	0.9818	0.9818	0	0.9602	0.9602	0	0.9302	0.9302	0

The + and − signs in Eq. (8) refer to the outgoing and incoming geodesics, respectively. In order to understand the motion of the test particle around SV BH one needs to evaluate the effective potential, which is straightforwardly worked out using Eq. (8). We can used following equations to calculate effective potential

$$\frac{1}{2}\dot{r}^2 + V_{\text{eff}} = 0, \tag{9}$$

$$V_{\text{eff}} = -\frac{(aL - (a^2 + r^2)E)^2 - \Delta(m_0^2 r^2 + (L - aE)^2)}{2r^4}. \tag{10}$$

The range of angular momentum for free falling particle, which is depicted in Tables 2 and 3 is calculated by following equations:

$$V_{\text{eff}} = 0 \text{ and } \frac{dV_{\text{eff}}}{dr}. \tag{11}$$

The lowest and the highest limits of angular momentum of falling geodesic is described with L_2, L_1 in Table 2 and L_4, L_3 in Table 3, respectively. In Fig. 6, the effective potential is shown by varying the angular momentum of the incoming test particle for a fixed a and l. it is observed that the potential barrier rises for greater values of L, which means a boosted particle can easily begin circling around the BH.

When observing a particle's geodesics in curved spacetime, the value of the particle's momentum is crucial. Thus, one may get the critical value of the angular momentum from Eq. (6) where for the time-like particles $\dot{t} \geq 0$, i.e. Equation (6) leads to

$$\frac{1}{r^2}\left[\frac{(a^2 + r^2)}{\Delta}(E(a^2 + r^2) - aL) + a\left(L - aE\right)\right] \geq 0. \tag{12}$$

When $r \to r_H^E$, the above condition reduces to

$$E - \Omega_H L \geq 0, \tag{13}$$

where $\Omega_H = \frac{a}{r_h^2 + a^2}$ is the angular velocity of the black hole at the horizon, and it is derived in Eq. (20). The critical angular momentum of the particle is defined by $L_c = E/\Omega_H$.

Figure 7 gives a comprehensible demonstration of the geodesics in this BH. It is numerically calculated that for the values of $l < l_*$ (where $l_* = 0.53948$), the particle with $L < L_c$ is always captured by the BH gravity and falls exactly at the horizon if $L = L_c$, however, when $L > L_c$ the geodesics never fall into the BH. But for the cases of $l > l_*$, the particle which is equipped with L_c cannot reach to the horizon. Meaning that turning points of this cases do not correspond to the event horizon.

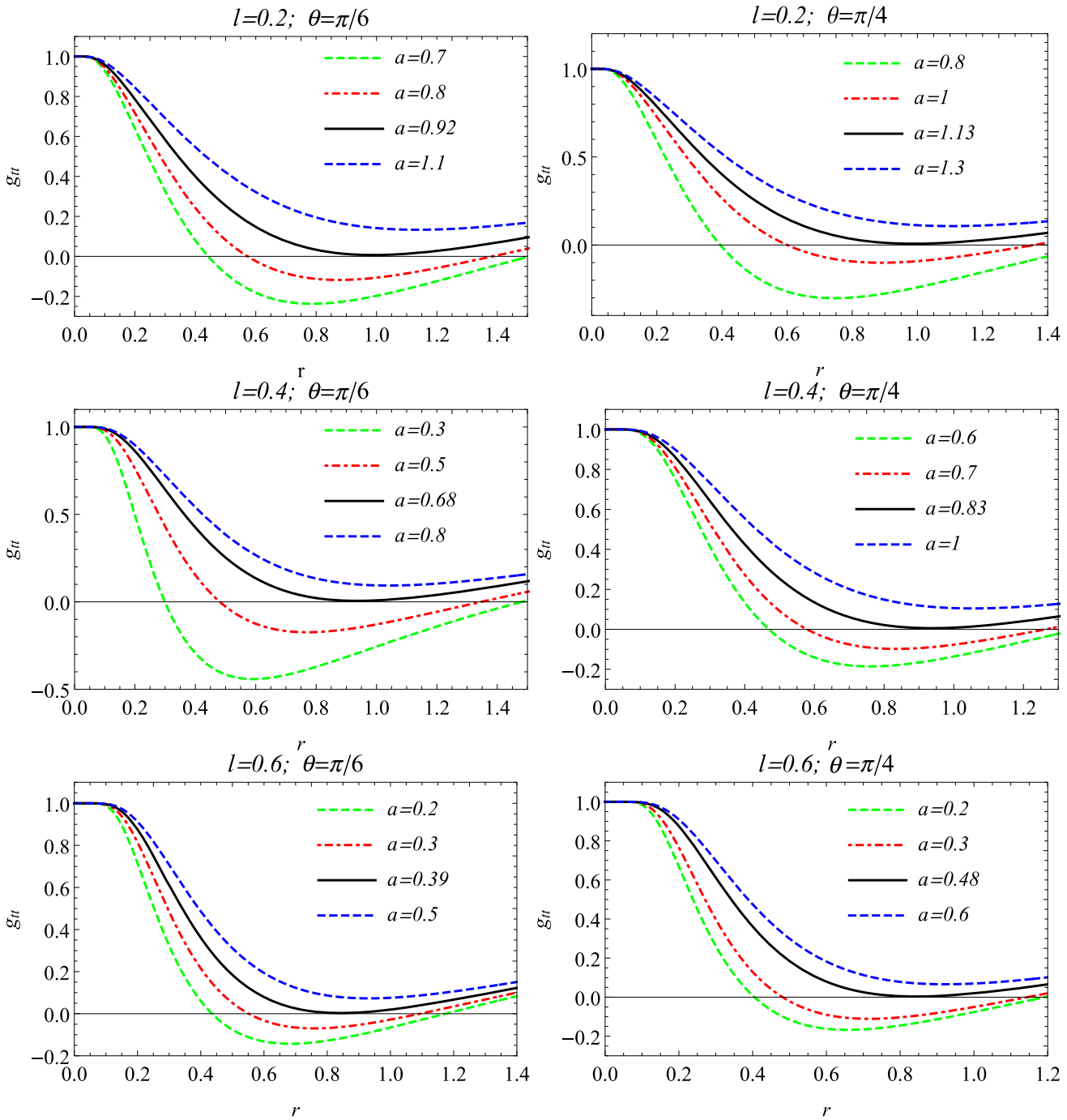

Fig. 4 Plot showing the variation of infinite redshift surface with different values of l, a and θ. Here $M = 1$

The solution to the simultaneous equations $\dot{r} = \partial_r V_{\text{eff}} = \partial_r^2 V_{\text{eff}} = 0$ defines the innermost stable circular orbit r_{ISCO} of the particle. It is difficult to find analytical solution of the radius of ISCO, but numerical analysis is given in Fig. 8, i.e., it illustrates the variation of r_{ISCO} with respect to a and l for the different cases. Furthermore, it can be easily noticed from these figures that the radius of the innermost stable circular orbit is sensible to the value of l and a. To be more precise, r_{ISCO} shows downward trend for both parameters.

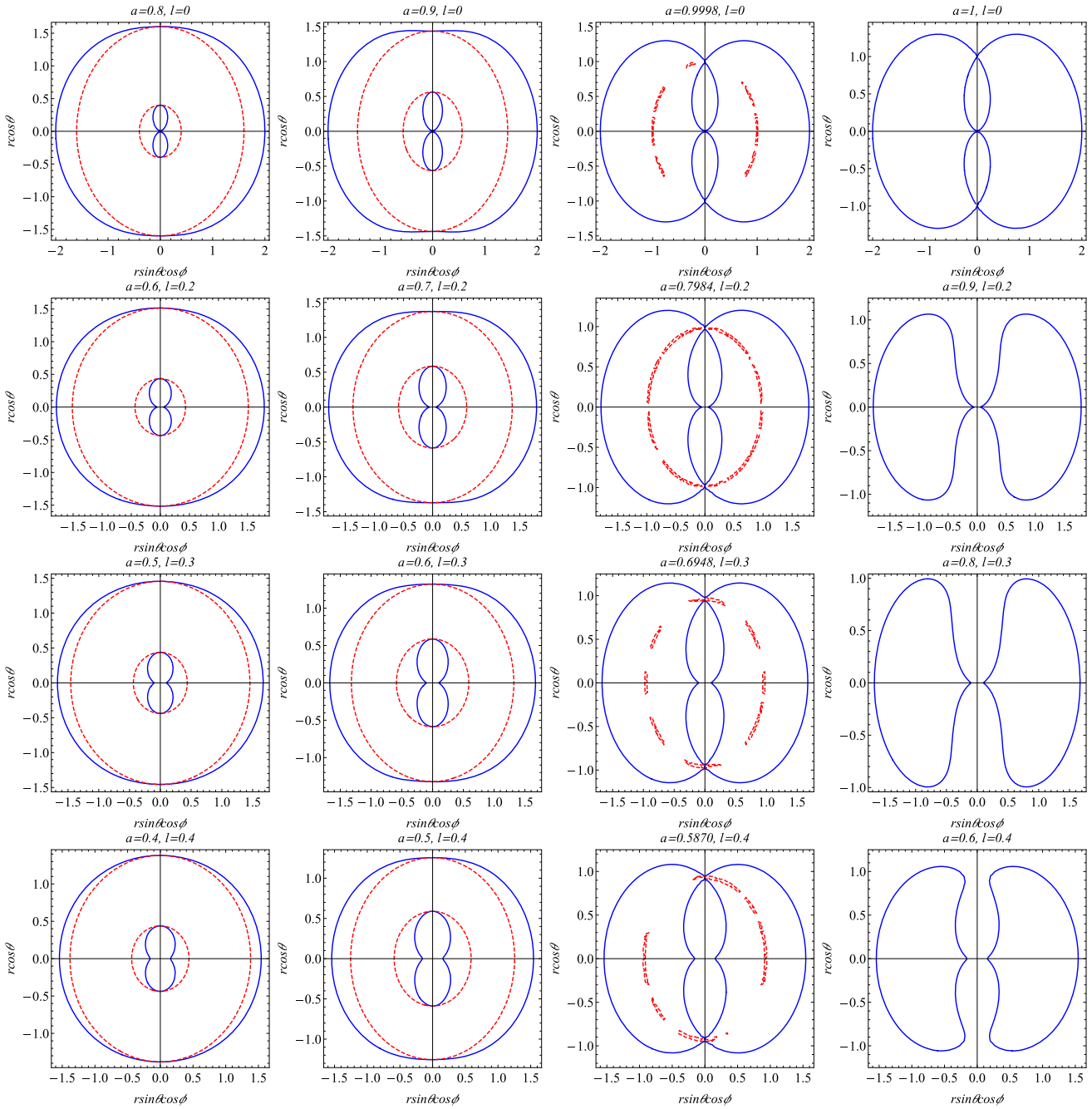

Fig. 5 Plot showing the variation of the shape of ergosphere for a rotating SV BH in xz-plane for the different values of a and l. The blue and the red lines correspond, respectively, to the static limit surfaces and horizons. The third row illustrates the merging of two event horizons. Here $M = 1$

4 Particle acceleration

In this section, we do an inclusive analysis to probe the acceleration of particles in the SV BH described by the spacetime metric (1). We accurately consider the center of mass (CM) energy produced due to a two-particle collision near the horizon considering an extremal and a non-extremal BHs in the Kerr-like spacetime. We put forth the scenario where two non-relativistic particles initially located at infinity at rest fall freely toward compact object and ultimately encounter a massive collision near the horizon. Here, we do a unique choice for the collision point because particles falling in from infinity appear with an infinite blue-shift at the horizon and hence are considered to produce an arbitrarily large amount of energy.

Table 2 The limiting values of angular momentum for different extremal cases. Here $l_* = 0.53948$ and $M = 1$

l	a_E	r_H^E	L_2	L_1	L_c
0	1.0	1.00000	−4.82843	2.00000	2.00000
0.2	0.79861076037439	0.98186	−4.52868	2.00578	2.00578
0.3	0.69505544577365	0.96026	−4.36208	2.02172	2.02172
0.4	0.58729623390243	0.93023	−4.17874	2.06069	2.06069
l_*	0.47204473678589	0.871887	−3.97046	2.15248	2.15248
0.6	0.34180530576217	0.83888	−3.71893	2.35355	2.40064
0.7	0.16598902588924	0.76850	−3.35378	2.66542	3.72407

Table 3 The limiting values of angular momentum for different non-extremal cases. Here $M = 1$

l	a_E	r_H^+	r_H^-	L_4	L_3	L_c'
0	0.9	1.43589	0.56411	−4.75680	2.63246	3.19115
0.2	0.6	1.51505	0.43488	−4.36638	2.89374	4.42563
0.3	0.5	1.45583	0.43828	−4.19068	2.89207	4.73888
0.4	0.4	1.38133	0.43857	−3.99933	2.88869	5.17018
0.5	0.3	1.28554	0.44231	−3.78700	2.88276	5.80871
0.6	0.2	1.15506	0.46592	−3.54427	2.87306	6.87081

4.1 Near horizon collision

Now we analyze the ultrahigh energy produced as a result of a two-particle collision near the horizon of SV BH. We consider particles with the same mass m_0 and different four-velocities u_1 and u_2. CM energy E_{CM} of collision between two particles at the radial coordinate r is given by the following expression [19, 46]

$$E_{CM} = m_0\sqrt{2}\sqrt{1 - g_{\mu\nu}u_1{}^{\mu}u_2{}^{\nu}}. \tag{14}$$

By substituting Eqs. (6)–(8) into the Eq. (14), we can easily obtain

$$\frac{E_{CM}^2}{2{m_0}^2} = \frac{e^{l/r}\mathcal{K}}{r^2\Delta}, \tag{15}$$

where $\mathcal{K}$ is defined in the following form

$$\begin{aligned}\mathcal{K} &= 2Mr(a - L_1)(a - L_2) - 2Mr^3 + r^2e^{l/r}\left(2a^2 - L_1L_2 + 2r^2\right)\\ &\quad - e^{l/r}\sqrt{\left(a^2 - aL_1 + r^2\right)^2 - \left(a^2 + r\left(r - 2Me^{-\frac{l}{r}}\right)\right)\left((a - L_1)^2 + m_0^2r^2\right)}\\ &\quad \times\sqrt{\left(a^2 - aL_2 + r^2\right)^2 - \left(a^2 + r\left(r - 2Me^{-\frac{l}{r}}\right)\right)\left((a - L_2)^2 + m_0^2r^2\right)}.\end{aligned} \tag{16}$$

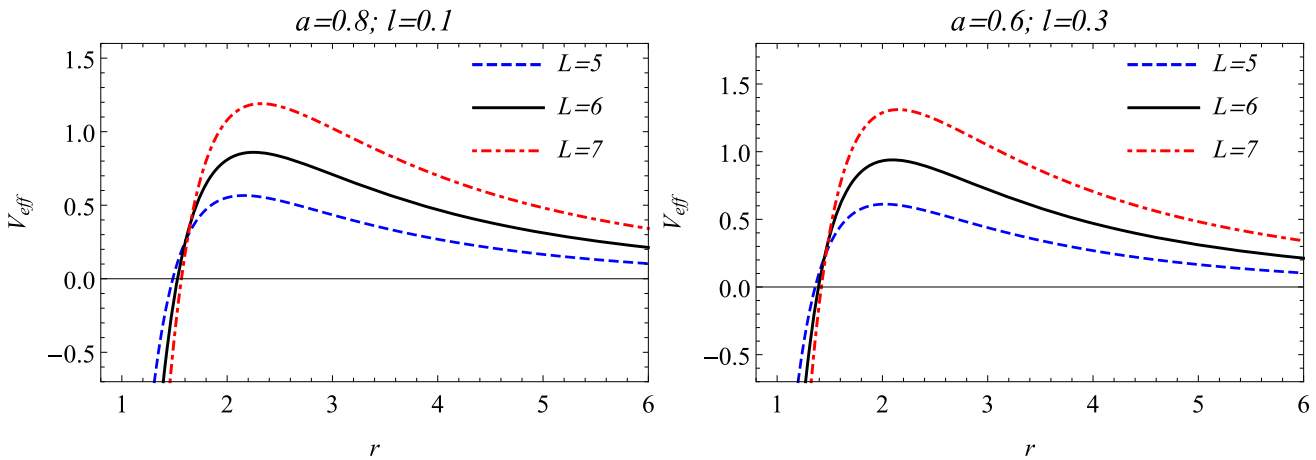

Fig. 6 Plot shows the behavior of V_{eff} versus r for different values of angular momentum, where $M = 1$

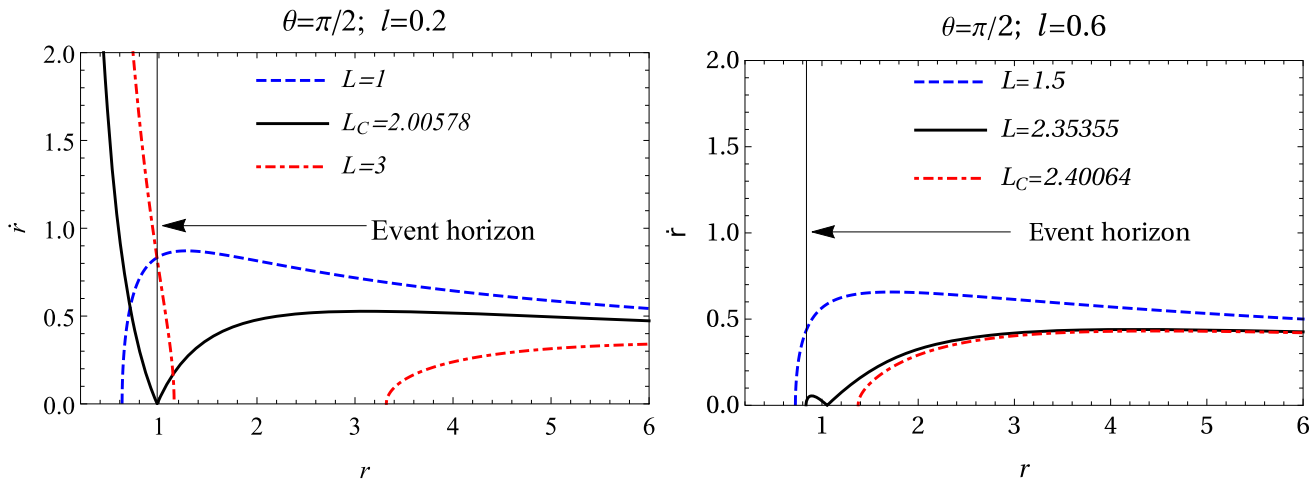

Fig. 7 The variation of $\dot{r}$ with respect to the radial coordinate for an extremal BH. In the left panel $a_E = 0.7986107603$ and in the right panel $a_E = 0.5872962339$. Here $M = 1$

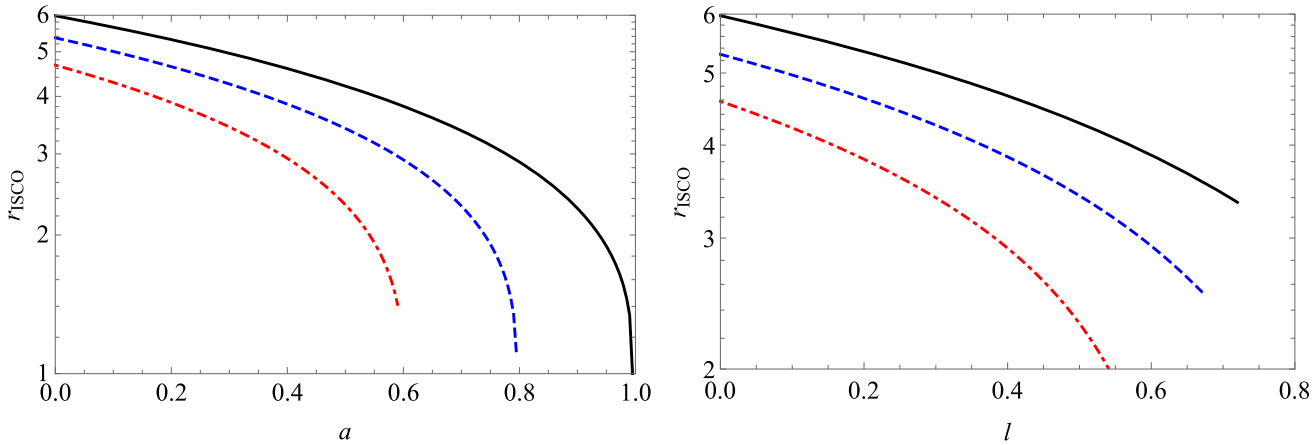

Fig. 8 The inner most stable circular orbits by varying a and l for various values of l and a. In the left-hand side, for the deviation parameter $l = 0$ (*black*), $l = 0.2$ (*blue*) and $l = 0.4$ (*red*). In the right-hand side, for the spin parameter $a = 0$ (*black*), $a = 0.2$ (*blue*) and $a = 0.4$ (*red*). Here $M = 1$

In our discussion, the participating particles have the same intrinsic identities and are mainly distinguished by their angular momenta L_1 and L_2. Here, for the sake of simplicity, we shall take the conserved energies E_1/m_0=E_2/m_0=1. Obviously as $r \to r_H^E$, Eq. (15) has indeterminate form when we choose numerical values of M, a, l and r_H^E. After applying l'Hospital's rule twice, it can be seen that if one of the particles has the critical angular momentum L_c, E_{CM} become infinite as $r \to r_H^E$. The expression of E_{CM} is too lengthy to write it here, but in general it is proportional to

$$\frac{E_{\rm CM}^2}{2m_0^2}\left(r \to r_H^E\right) \sim \frac{1}{(L_1 - L_c)^{3/2}(L_2 - L_c)^{3/2}}. \tag{17}$$

It is worth to mention that an arbitrarily high amount of energy is obtained when the test particle approaching the black hole has the critical angular momentum L_c. The limiting values of the angular momentum along with the corresponding spin of the BH, deviation parameters l and radius of the event horizon for the *extremal* case are presented, as shown in the Table 2. The E_{CM} generated as a result of collision near the horizon of an extremal BH for different values of l is shown in Fig. 9. From the Table 2 and Fig. 9, we can conclude that for the smaller values of deviation parameter, the CM energy instantaneously diverges near the horizon whenever the incoming particle is equipped with the critical parameters of the motion. And for the larger values of l ($l > l_*$), particles, which has critical angular momentum cannot reach to the horizon and infinite amount of CM energy cannot be produced. Additionally the particles admitting $L < L_c$ contribute only a finite E_{CM} too.

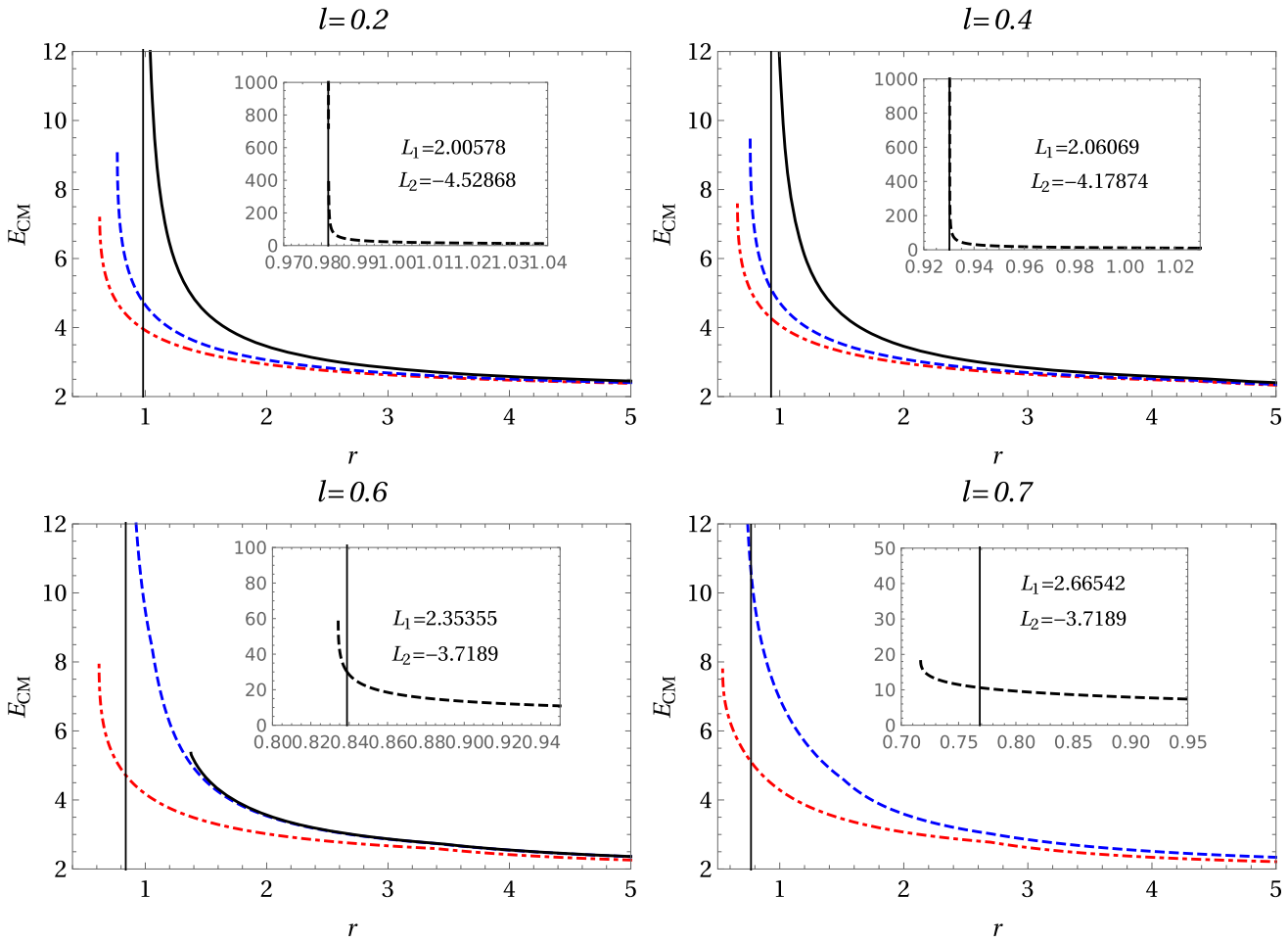

Fig. 9 Plot shows dependence of the center-of-mass energy $E_{c.m}$ to radial coordinate r for an extremal BH in different values of l. In the top left-hand corner, for the deviation parameter l=0.2, spin a_E=0.798610, angular momentum L_1=2.00578 (*black*), 1.3 (*blue*), 1 (*red*) and L_2=−4.52868. In the top right-hand corner, for the deviation parameter l=0.4, spin a_E=0.58729, angular momentum L_1=2.06069 (*black*), 1.3 (*blue*), 1 (*red*) and L_2=−4.17874. In the bottom left-hand corner, for the deviation parameter l=0.6, spin a_E=0.341805, angular momentum L_1=2.40064 (*black*), 2.35355 (*blue*), 1 (*red*) and L_2=−4.52868. In the bottom right-hand corner, for the deviation parameter l=0.7, spin a_E=0.165989, angular momentum L_1=3.72407 (*black* which is stopped before 5 radial coordinate), 2.66542 (*blue*), 1 (*red*) and L_2=−4.17874. Here $M = 1$

4.2 Near horizon collision in non-extremal SV BH

We also study the properties of E_{CM} in the limit $r \to r_H^+$ of non-extremal BH. Again after applying l'Hospital's rule twice, the expression of E_{CM} is proportional to

$$\frac{E_{\rm CM}^2}{2m_0^2}(r \to r_H^+) \sim \frac{1}{(L_1 - L_c')(L_2 - L_c')}. \tag{18}$$

The Eq. (18) tells us that E_{CM} can be infinite if L_1 or L_2 is equal to L_c'. But critical value of angular momentum is not in the acceptable range in non-extremal BH case. For example in the case of $l = 0.2$, $a = 0.6$ and $r_H^+ = 1.51505$, the critical value of angular momentum is calculated as $L_c' = 4.4256$ which is not in the acceptable range. The limiting values of the angular momentum along with the corresponding spin, deviation parameters and the horizons for the *non-extremal* are presented in the Table 3. From the Table 3, one can conclude that angular momentum of free falling particle can never be equal to the critical value of it for non-extremal BH, which means in non-extremal cases the center of mass energy is finite. Figure 10 shows a visualization of this process. In general, if we consider a collision in a non-extremal space-time background, we attain a limited E_{CM} irrespective of the event's location (see Fig. 10).

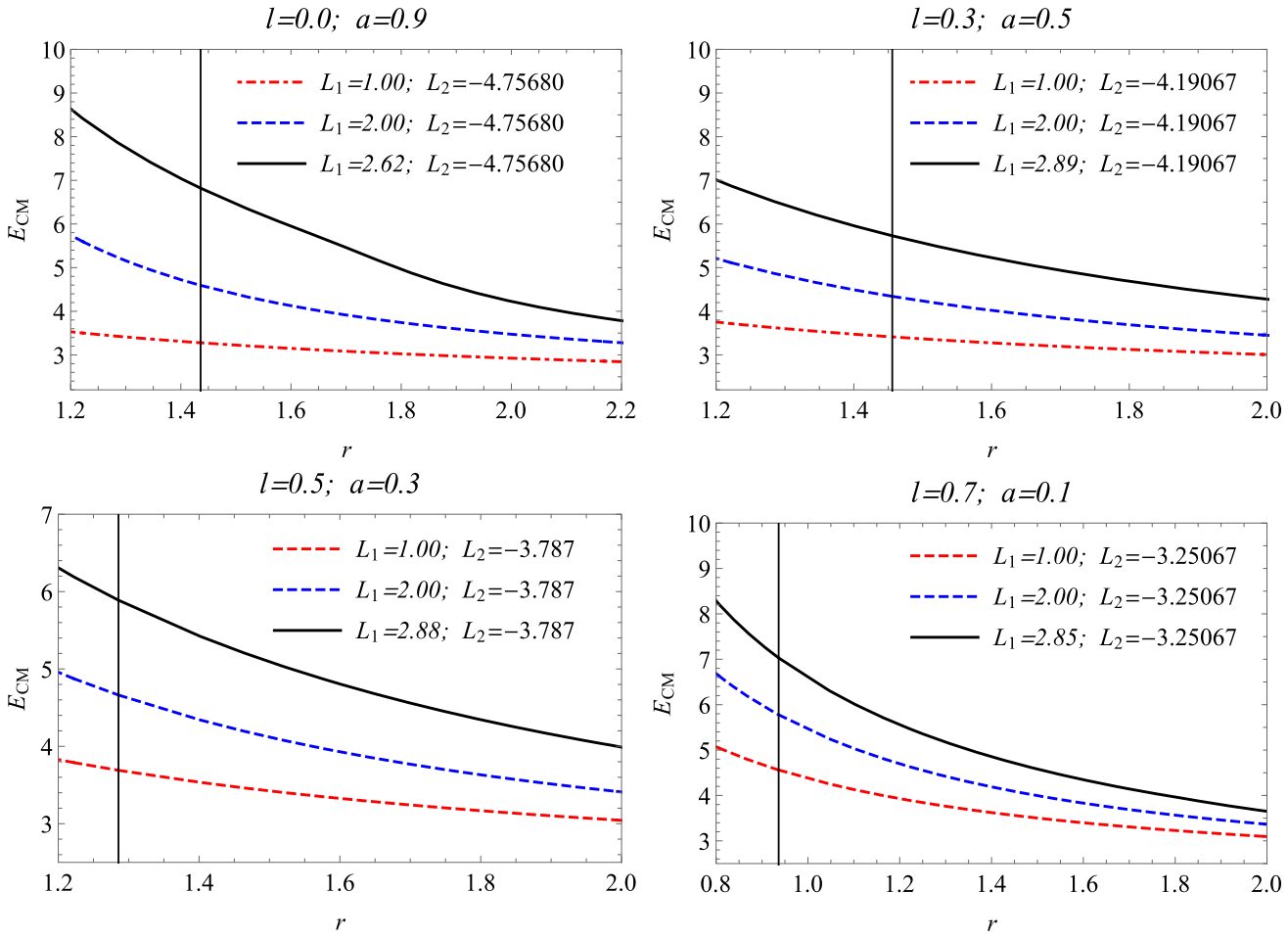

Fig. 10 Plot showing the behavior of the center-of-mass energy $E_{\mathrm{c.m}}$ versus the radial coordinate r for a non-extremal BH. Here $M = 1$

5 Thermodynamics of SV BH

In this section, we analyze thermodynamics of this BH in SV BH. General form of metric can be written as

$$ds^2 = g_{tt}dt^2 + g_{rr}dr^2 + g_{\theta\theta}d\theta^2 + g_{\phi\phi}d\phi^2 + 2g_{t\phi}dtd\phi. \tag{19}$$

The angular velocity of a test particle at the event horizon, with vanishing angular momentum, can be calculated using the formula $\Omega_H = -g_{t\phi}/g_{\phi\phi}$ for the rotating Kerr-like BH

$$\Omega_H = \frac{a}{r_h^2 + a^2}. \tag{20}$$

We will use the expression (20) for our further calculations. Now we turn to calculate thermodynamical quantities of SV BH. The BH mass (M, which is equal to enthalpy (H)) can be derived by making Eq. (3) equals to zero. As a result one may obtain

$$M = \frac{(a^2 + r_h^2)e^{\frac{l}{r_h}}}{2r_h}. \tag{21}$$

Figure 11 demonstrates the enthalpy as a function of r_h. One may see that an increase in the parameters a and l corresponds to greater mass (enthalpy) for fixed r_h. And also using well-known formula $T = \frac{\kappa}{2\pi}$, one can get Hawking temperature for this type of BH, where κ is the surface gravity of rotating BH and we can calculate it with following expression [66, 67]

$$\kappa = \frac{1}{2}\sqrt{(g^{rr})'(G_{tt})'}, \tag{22}$$

where

$$G_{tt} = -g_{tt} - 2g_{t\phi}\Omega_H - g_{\phi\phi}\Omega_H^2, \tag{23}$$

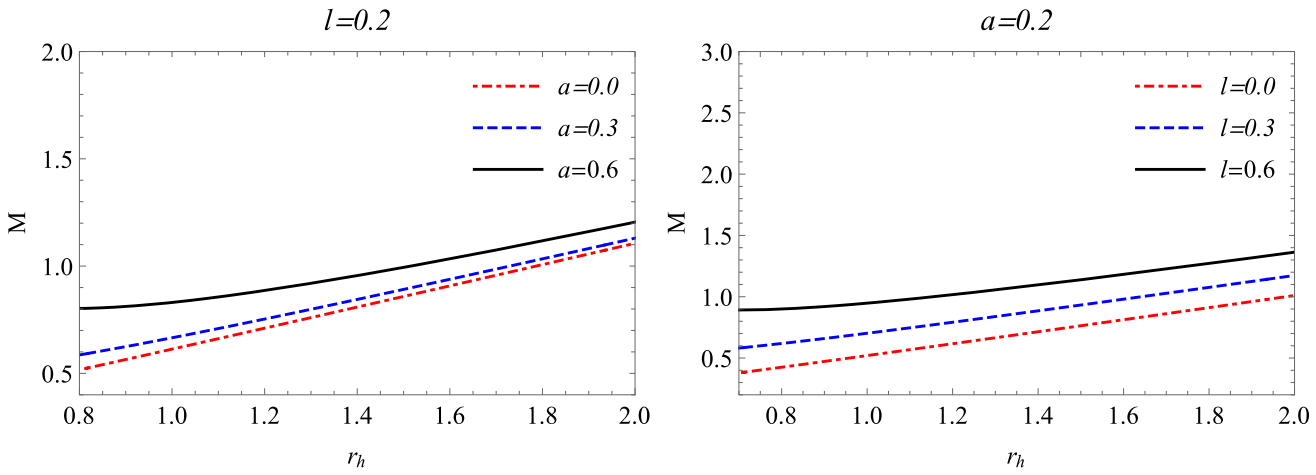

Fig. 11 Plot show the variation of enthalpy with respect to horizon radius. Here $M = 1$

and $(g^{rr})'$, $(G_{tt})'$ means derivative of g^{rr}, G_{tt} with respect to r, respectively. Eventually the final expression for temperature looks

$$T = \frac{(r_h - l)r_h^2 - (l + r_h)a^2}{4\pi r_h^2\left(a^2 + r_h^2\right)}. \tag{24}$$

It is easy to see that one can recover temperature formula for Kerr BH by taking $l = 0$, and also can recover temperature formula for Schwarzschild BH by taking $l = 0$, & $a = 0$. With the help of Eq. (24), one can depict this result visually. Figure 12 shows temperature dependency on the radius of event horizon for different values of l and a in Kerr-like spacetime. We can notice from this picture that deviation parameter 'cools down' BH. Precisely speaking, an increase of l causes temperature to decrease like spin parameter a if keep radius of horizon unchanged. Now one calculates area and entropy of Ker-like BH using the following general expression [67]

$$A = \int_0^{2\pi}\int_0^{\pi}\sqrt{g_{\theta\theta}g_{\phi\phi}}d\theta d\phi = 4\pi\left(a^2 + r_h^2\right), \tag{25}$$

and obtain [68]

$$S = \frac{A}{4} = \pi\left(a^2 + r_h^2\right). \tag{26}$$

Although area of outer event horizon and entropy does not depend on the deviation parameter explicitly, radius of event horizon depends on it. It means that deviation parameter somehow reduces the area, as well as the entropy. We will use Eqs. (24)–(21) and (26) to define the expression of Gibbs free energy as [68, 69]

$$\begin{aligned} G &= M - TS \\ &= \frac{a^2\left[r_h\left(e^{\frac{l}{r_h}} + 2\right) + 2l\right] + r_h^2\left[r_h\left(e^{\frac{l}{r_h}} - 2\right) + 2l\right]}{2r_h^2}. \end{aligned} \tag{27}$$

From Eq. (27) one can observe that Gibbs energy is positive in the vicinity of $r_h = 0$, i.e., for small black holes are stable but the black holes are unstable at larger horizon radius. Furthermore, it is clear that both parameters (l an a) cause Gibbs energy to increase.

The phenomenon characterized by the creation and annihilation of an abundant quantity of particles in immediate proximity to the black hole's event horizon is denoted as emission energy. Quantum fluctuations transpiring within the internal regions of black holes constitute the fundamental origin of this energy manifestation. The main reason for the BH evaporation within a certain period is due to the positive-energy particles that tunnel out of the BH in the core area where Hawking radiation occurs. Now we consider the energy emission rate BH with SV parameter. The absorption cross-section often oscillates around a limiting constant value σ_{lim}. The limiting value of cross-section σ_{lim} is depended to the event horizon's radius as following [65, 71]

$$\sigma_{lim} \approx \pi r_h^2. \tag{28}$$

The expression of the emission energy rate from the BH as [65, 71]

$$\frac{d^2\mathcal{E}}{d\omega dt} = \frac{2\pi^2\sigma_{lim}}{e^{\frac{\omega}{T}} - 1}\omega^3. \tag{29}$$

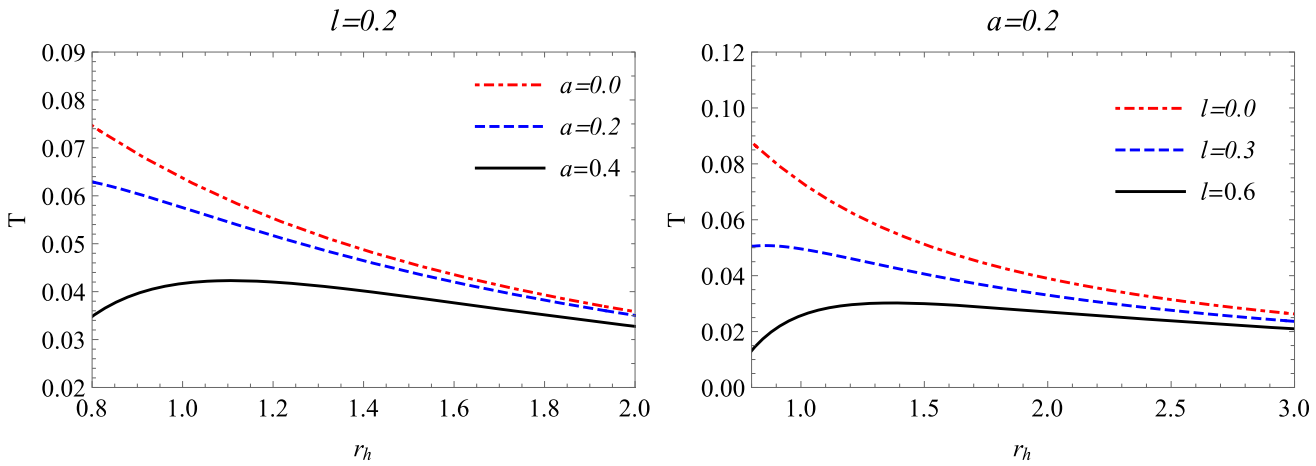

Fig. 12 Plot shows the variation of temperature with horizon radius. Here $M = 1$

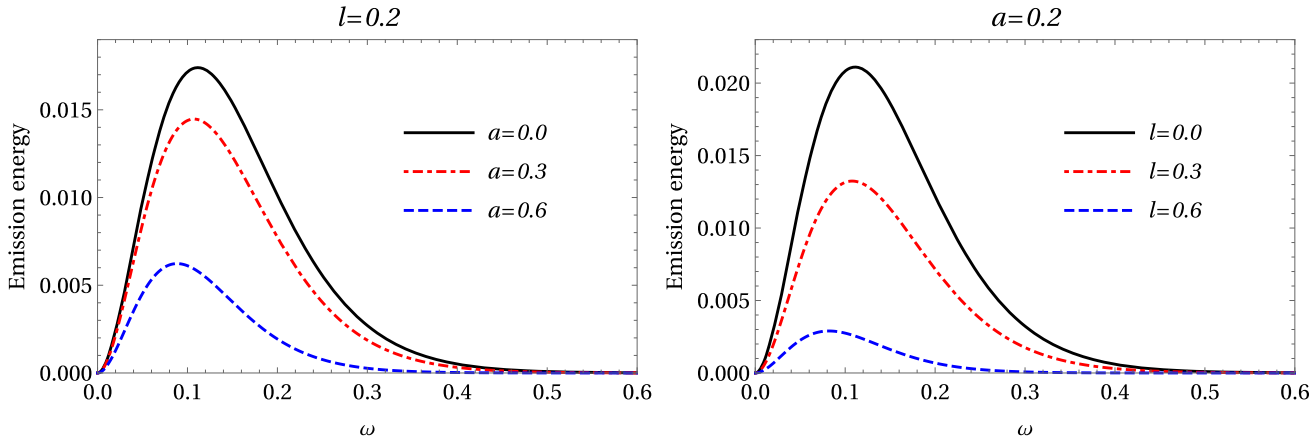

Fig. 13 Plot shows the variation of temperature with horizon radius. Here $M = 1$

Where T is the Hawking temperature. The energy emission rate is represented in Fig. 13 as a function of ω for different values of the deviation parameter (right panel) and spin parameter (left panel). From this figure, one can see that there exists a peak of the energy emission rate for the black hole. When these parameters increase, the peak decreases and shifts to the low frequency. Also one can notice that the variation of l has a stronger effect on the emission of particles around the black hole.

6 Conclusion

In this paper, we constructed an insightful discussion regarding the rotating BH's structure, circular orbits, center-of-mass energy and thermodynamics in rotating SV spacetime. So, we have obtained following results:

- First, we have obtained border between BH and naked singularity using their parameters in Fig. 1.
- If the value of parameters is lower than their extremal values, there exist Cauchy and event horizon in Figs. 2 and 3. When these two parameters l and a of the spacetime reach to their extremal values, these two horizons merge, and also no horizon for $a > a_E$ and $l > l_E$.
- The growth of parameters l and a in SV gravity affects positively to the thickness of ergosphere of the BH, meaning that it becomes thicker.
- Within this work the radius of ISCO is also discussed in SV spacetime with its parameters l and a. A rise in these parameters make ISCO radius smaller, and it is represented in Fig. 8.
- Using massive particles orbits, we checked energy extraction from BH for extremal and non-extremal case through BSW effect. Center-of-mass energy can be arbitrarily high for the extremal SV BH, which is not true for non-extremal SV BH.
- Properties of thermodynamics are studied for different cases: enthalpy, hawking temperature, entropy and Gibbs free energy. To be more precise, an increase of BH's parameters l and a also cause Gibbs free energy to increase. An opposite is true for the temperature of this type of BH. Area and entropy of Kerr-like (or rotating SV) BH are also non-explicitly depend on these

parameters and their effect make the entropy smaller. To get more information about them, we plotted several graphs of quantities of thermodynamics.

- Plots of the energy emission rate with respect to frequency ω are drawn for different values of l and a parameters. An effect of deviation parameter l is more noticeable.

Acknowledgements This research is partly supported by Research Grant F-FA-2021-510 of the Uzbekistan Ministry for Innovative Development.

Data Availability Statement This manuscript has no associated data or the data will not be deposited.

References

1. F.W. Dyson, A.S. Eddington, C. Davidson, Philos. Trans. R. Soc. Londn. Ser. A **220**, 291 (1920). https://doi.org/10.1098/rsta.1920.0009
2. B. Patla and R. J. Nemiroff, Astrophys. J **685**, 1297 (2008), http://arxiv.org/abs/0711.4811 arXiv:0711.4811 [astro-ph] https://doi.org/10.1086/588805
3. A. Einstein, Sitzungsberichte der K öniglich Preussischen Akademie der Wissenschaften , 778 (1915)
4. C. M. Will, Living Reviews in Relativity **9**, 3 (2006), http://arxiv.org/abs/gr-qc/0510072 arXiv:gr-qc/0510072 [gr-qc]https://doi.org/10.12942/lrr-2006-3
5. B. P. Abbott, LIGO Scientific Collaboration, and Virgo Collaboration, Phys. Rev. Lett. **116**, 061102 (2016), http://arxiv.org/abs/1602.03837 arXiv:1602.03837 [gr-qc] https://doi.org/10.1103/PhysRevLett.116.061102
6. K. Akiyama and et al. (Event Horizon Telescope Collaboration), Astrophys. J. **875**, L1 (2019), http://arxiv.org/abs/1906.11238 arXiv:1906.11238 [astro-ph.GA] https://doi.org/10.3847/2041-8213/ab0ec7
7. K. Akiyama et al., Astrophys. J. Lett. **930**, L12 (2022). https://doi.org/10.3847/2041-8213/ac6674
8. A. Tripathi, Y. Zhang, A. B. Abdikamalov, D. Ayzenberg, C. Bambi, J. Jiang, H. Liu, and M. Zhou, Astrophys. J. **913**, 79 (2021), arXiv:2012.10669 [astro-ph.HE] https://doi.org/10.3847/1538-4357/abf6cd
9. A. Tripathi, S. Nampalliwar, A. B. Abdikamalov, D. Ayzenberg, C. Bambi, T. Dauser, J. A. García, and A. Marinucci, Astrophys. J. **875**, 56 (2019), arXiv:1811.08148 [gr-qc] https://doi.org/10.3847/1538-4357/ab0e7e
10. C. Bambi, Phys. Rev. D **87**, 023007 (2013), arXiv:1211.2513 [gr-qc] https://doi.org/10.1103/PhysRevD.87.023007
11. Z. Li, L. Kong, and C. Bambi, Astrophys. J. **787**, 152 (2014), arXiv:1401.1282 [gr-qc] https://doi.org/10.1088/0004-637X/787/2/152
12. T. Johannsen and D. Psaltis, Astrophys. J. **716**, 187 (2010a), arXiv:1003.3415 [astro-ph.HE] https://doi.org/10.1088/0004-637X/716/1/187
13. T. Johannsen and D. Psaltis, Astrophys. J. **718**, 446 (2010b), arXiv:1005.1931 [astro-ph.HE] https://doi.org/10.1088/0004-637X/718/1/446
14. A. Simpson, M. Visser, Phys. Rev. D **105**, 064065 (2022). https://doi.org/10.1103/PhysRevD.105.064065
15. F. Sarikulov, F. Atamurotov, A. Abdujabbarov, B. Ahmedov, Eur. Phys. J. C **82**, 771 (2022). https://doi.org/10.1140/epjc/s10052-022-10711-4
16. A. Simpson and M. Visser, Universe **6**, 8 (2019), arXiv:1911.01020 [gr-qc] https://doi.org/10.3390/universe6010008
17. T. Berry, A. Simpson, and M. Visser, Universe **7**, 2 (2020), arXiv:2008.13308 [gr-qc] https://doi.org/10.3390/universe7010002
18. F. Atamurotov, F. Sarikulov, V. Khamidov, A. Abdujabbarov, Eur. Phys. J. Plus **137**, 567 (2022). https://doi.org/10.1140/epjp/s13360-022-02780-x
19. M. Bañados, J. Silk, S.M. West, Phys. Rev. Lett. **103**, 111102 (2009). https://doi.org/10.1103/PhysRevLett.103.111102
20. A. Jawad, F. Ali, M. Jamil, and U. Debnath, Commun. Theor. Phys. **66**, 509 (2016), arXiv:1610.07411 [gr-qc] https://doi.org/10.1088/0253-6102/66/5/509
21. S. Hussain and M. Jamil, Phys. Rev. D **92**, 043008 (2015), arXiv:1508.02123 [gr-qc] https://doi.org/10.1103/PhysRevD.92.043008
22. G. Z. Babar, M. Jamil, and Y.-K. Lim, Int. J. Mod. Phys. D **25**, 1650024 (2016), arXiv:1504.00072 [gr-qc] https://doi.org/10.1142/S0218271816500243
23. A. Zakria and M. Jamil, J. High Energy Phys. **2015**, 147 (2015), arXiv:1501.06306 [gr-qc] https://doi.org/10.1007/JHEP05(2015)147
24. I. Brevik and M. Jamil, Int. J. Geometr. Methods Mod. Phys. **16**, 1950030 (2019), arXiv:1901.00002 [gr-qc] https://doi.org/10.1142/S0219887819500300
25. S. Chen, M. Wang, and J. Jing, J. High Energy Phys. **2016**, 82 (2016), arXiv:1604.02785 [gr-qc] https://doi.org/10.1007/JHEP09(2016)082
26. K. Hashimoto and N. Tanahashi, Phys. Rev. D **95**, 024007 (2017), arXiv:1610.06070 [hep-th] https://doi.org/10.1103/PhysRevD.95.024007
27. W. Han, Gen. Relativity Gravit. **40**, 1831 (2008), arXiv:1006.2229 [gr-qc] https://doi.org/10.1007/s10714-007-0598-9
28. R.M. Wald, Phys. Rev. D. **10**, 1680 (1974). https://doi.org/10.1103/PhysRevD.10.1680
29. A.N. Aliev, N. Özdemir, Mon. Not. R. Astron. Soc. **336**, 241 (2002). https://doi.org/10.1046/j.1365-8711.2002.05727.x. arXiv:gr-qc/0208025
30. Z. Stuchlík, J. Schee, A. Abdujabbarov, Phys. Rev. D **89**, 104048 (2014). https://doi.org/10.1103/PhysRevD.89.104048
31. A. Abdujabbarov and B. Ahmedov, Phys. Rev. D **81**, 044022 (2010), arXiv:0905.2730 [gr-qc] https://doi.org/10.1103/PhysRevD.81.044022
32. A. Abdujabbarov, B. Ahmedov, and A. Hakimov, Phys.Rev. D **83**, 044053 (2011a), http://arxiv.org/abs/1101.4741 arXiv:1101.4741 [gr-qc] https://doi.org/10.1103/PhysRevD.83.044053
33. A. A. Abdujabbarov, B. J. Ahmedov, S. R. Shaymatov, and A. S. Rakhmatov, Astrophys. Space Sci. **334**, 237 (2011b), http://arxiv.org/abs/1105.1910 arXiv:1105.1910 [astro-ph.SR] https://doi.org/10.1007/s10509-011-0740-8
34. Z. Stuchlík and M. Kološ, Eur. Phys. J. C **76**, 32 (2016), http://arxiv.org/abs/1511.02936 arXiv:1511.02936 [gr-qc] https://doi.org/10.1140/epjc/s10052-015-3862-2
35. J. Kovář, O. Kopáček, V. Karas, and Z. Stuchlík, Class. Quant. Gravity **27**, 135006 (2010), http://arxiv.org/abs/1005.3270 arXiv:1005.3270 [astro-ph.HE] https://doi.org/10.1088/0264-9381/27/13/135006
36. J. Kovář, P. Slaný, C. Cremaschini, Z. Stuchlík, V. Karas, and A. Trova, Phys. Rev. D **90**, 044029 (2014), http://arxiv.org/abs/1409.0418 arXiv:1409.0418 [gr-qc] https://doi.org/10.1103/PhysRevD.90.044029
37. F. de Felice, F. Sorge, Class. Quant. Gravity **20**, 469 (2003)
38. F. de Felice, F. Sorge, S. Zilio, Class. Quant. Gravity **21**, 961 (2004). https://doi.org/10.1088/0264-9381/21/4/016
39. J. Rayimbaev, A. Abdujabbarov, M. Jamil, and W.-B. Han, Nuclear Phys. B **966**, 115364 (2021), http://arxiv.org/abs/2009.04898 arXiv:2009.04898 [gr-qc] https://doi.org/10.1016/j.nuclphysb.2021.115364
40. A. Abdujabbarov, J. Rayimbaev, B. Turimov, F. Atamurotov, Phys. Dark Univ. **30**, 100715 (2020). https://doi.org/10.1016/j.dark.2020.100715
41. B. Narzilloev, J. Rayimbaev, S. Shaymatov, A. Abdujabbarov, B. Ahmedov, and C. Bambi, Phys. Rev. D **102**, 044013 (2020), http://arxiv.org/abs/2007.12462 arXiv:2007.12462 [gr-qc] https://doi.org/10.1103/PhysRevD.102.044013
42. J. Vrba, A. Abdujabbarov, M. Kološ, B. Ahmedov, Z. Stuchlík, J. Rayimbaev, Phys. Rev. D **101**, 124039 (2020). https://doi.org/10.1103/PhysRevD.101.124039
43. O. B. Zaslavskii, Phys. Rev. D **82**, 083004 (2010), http://arxiv.org/abs/1007.3678 arXiv:1007.3678 [gr-qc] https://doi.org/10.1103/PhysRevD.82.083004

44. O. B. Zaslavskii, Phys. Rev. D **86**, 084030 (2012a), http://arxiv.org/abs/1205.4410 arXiv:1205.4410 [gr-qc] https://doi.org/10.1103/PhysRevD.86.084030
45. O. B. Zaslavskii, Phys. Rev. D **85**, 024029 (2012b), http://arxiv.org/abs/1110.5838 arXiv:1110.5838 [gr-qc] https://doi.org/10.1103/PhysRevD.85.024029
46. G. Z. Babar, F. Atamurotov, S. Ul Islam, and S. G. Ghosh, Phys. Rev. D **103**, 084057 (2021), http://arxiv.org/abs/2104.00714 arXiv:2104.00714 [gr-qc] https://doi.org/10.1103/PhysRevD.103.084057
47. A. Tursunov, M. Kološ, A. Abdujabbarov, B. Ahmedov, and Z. Stuchlík, Phys. Rev. D **88**, 124001 (2013), http://arxiv.org/abs/1311.1751 arXiv:1311.1751 [gr-qc] https://doi.org/10.1103/PhysRevD.88.124001
48. A. Abdujabbarov, F. Atamurotov, N. Dadhich, B. Ahmedov, and Z. Stuchlik, Eur. Phys. J. C **75**, 399 (2015), http://arxiv.org/abs/1508.00331 arXiv:1508.00331 [gr-qc] https://doi.org/10.1140/epjc/s10052-015-3604-5
49. V. P. Frolov and A. A. Shoom, Phys. Rev. D. **82**, 084034 (2010), http://arxiv.org/abs/1008.2985 arXiv:1008.2985 [gr-qc] https://doi.org/10.1103/PhysRevD.82.084034
50. V. P. Frolov, Phys. Rev. D. **85**, 024020 (2012), http://arxiv.org/abs/1110.6274 arXiv:1110.6274 [gr-qc] https://doi.org/10.1103/PhysRevD.85.024020
51. A. Tursunov, M. Kološ, Z. Stuchlík, and D. V. Gal'tsov, Astrophys. J **861**, 2 (2018), http://arxiv.org/abs/1803.09682 arXiv:1803.09682 [gr-qc] https://doi.org/10.3847/1538-4357/aac7c5
52. A. Tursunov, B. Juraev, Z. Stuchlík, and M. Kološ, Phys. Rev. D **104**, 084099 (2021), http://arxiv.org/abs/2109.10288 arXiv:2109.10288 [gr-qc] https://doi.org/10.1103/PhysRevD.104.084099
53. N. Dadhich, A. Tursunov, B. Ahmedov, and Z. Stuchlík, Mon. Not. R. Astron. Soc **478**, L89 (2018), http://arxiv.org/abs/1804.09679 arXiv:1804.09679 [astro-ph.HE] https://doi.org/10.1093/mnrasl/sly073
54. S.W. Hawking, Commun. Math. Phys. **25**, 152 (1972). https://doi.org/10.1007/BF01877517
55. J.M. Bardeen, B. Carter, S.W. Hawking, Commun. Math. Phys. **31**, 161 (1973). https://doi.org/10.1007/BF01645742
56. J.D. Bekenstein, Phys. Rev. D **7**, 2333 (1973). https://doi.org/10.1103/PhysRevD.7.2333
57. S.W. Hawking, Commun. Math. Phys. **43**, 199 (1975). https://doi.org/10.1007/BF02345020
58. S.W. Hawking, Commun. Math. Phys. **46**, 206 (1976). https://doi.org/10.1007/BF01608497
59. R. M. Wald, Living. Rev. Rel. **4**, 6 (2001), http://arxiv.org/abs/gr-qc/9912119 arXiv:gr-qc/9912119 [gr-qc] https://doi.org/10.12942/lrr-2001-6
60. M.R.R. Good, Y.C. Ong, Eur. Phys. J. C **80**, 1169 (2020). https://doi.org/10.1140/epjc/s10052-020-08761-7
61. Y. S. Myung, Y.-W. Kim, and Y.-J. Park, Gen. Relat. Gravit. **41**, 1051 (2009), http://arxiv.org/abs/0708.3145 arXiv:0708.3145 [gr-qc] https://doi.org/10.1007/s10714-008-0690-9
62. K. Ghaderi, B. Malakolkalami, Astrophys. Space Sci. **361**, 161 (2016). https://doi.org/10.1007/s10509-016-2744-x
63. M. B. Jahani Poshteh and R. B. Mann, Phys. Rev. D **103**, 104024 (2021), http://arxiv.org/abs/2103.04365 arXiv:2103.04365 [hep-th] https://doi.org/10.1103/PhysRevD.103.104024
64. R.-G. Cai, L.-M. Cao, and N. Ohta, Phys. Lett. B **679**, 504 (2009), http://arxiv.org/abs/0905.0751 arXiv:0905.0751 [hep-th] https://doi.org/10.1016/j.physletb.2009.07.075
65. A. Ditta, X. Tiecheng, G. Mustafa, M. Yasir, F. Atamurotov, Eur. Phys. J. C **82**, 756 (2022). https://doi.org/10.1140/epjc/s10052-022-10708-z
66. A. Fatima and K. Saifullah, Astrophys. Space. Sci. **341**, 437 (2012), http://arxiv.org/abs/1108.1622 arXiv:1108.1622 [gr-qc] https://doi.org/10.1007/s10509-012-1098-2
67. S. H. Hendi, S. Hajkhalili, M. Jamil, and M. Momennia, Eur. Physi. J. C **81**, 1112 (2021), http://arxiv.org/abs/2111.10117 arXiv:2111.10117 [gr-qc] https://doi.org/10.1140/epjc/s10052-021-09836-9
68. S. Mahapatra and I. Banerjee, Phys. Dark Univ. **39**, 101172 (2023), http://arxiv.org/abs/2208.05796 arXiv:2208.05796 [gr-qc] https://doi.org/10.1016/j.dark.2023.101172
69. D. V. Singh, S. Upadhyay, and M. S. Ali, Int. J. Mod. Phys. A **37**, 2250049 (2022), http://arxiv.org/abs/2206.05057 arXiv:2206.05057 [gr-qc] https://doi.org/10.1142/S0217751X2250049X
70. M. Yasir, X. Tiecheng, A. Ditta, R. Ali, F. Atamurotov, New Astron. **105**, 102106 (2024). https://doi.org/10.1016/j.newast.2023.102106
71. A. Ditta, X. Tiecheng, R. Ali, F. Atamurotov, A. Mahmood, S. Mumtaz, Ann. Phys. **453**, 169326 (2023). https://doi.org/10.1016/j.aop.2023.169326
72. F. Javed, G. Mustafa, S. Mumtaz, F. Atamurotov, Nucl. Phys. B **990**, 116180 (2023). https://doi.org/10.1016/j.nuclphysb.2023.116180